

RESEARCH

Open Access



Biokinetics of subacutely co-inhaled same size gold and silver nanoparticles

Philku Lee¹, Jin Kwon Kim², Mi Seong Jo², Hoi Pin Kim², Kangho Ahn³, Jung Duck Park⁴, Mary Gulumian^{5,6}, Günter Oberdörster^{7*} and Il Je Yu^{2*}

Abstract

Background Toxicokinetics of nanomaterials, including studies on the absorption, distribution, metabolism, and elimination of nanomaterials, are essential in assessing their potential health effects. The fate of nanomaterials after inhalation exposure to multiple nanomaterials is not clearly understood.

Methods Male Sprague–Dawley rats were exposed to similar sizes of silver nanoparticles (AgNPs, 10.86 nm) and gold nanoparticles (AuNPs, 10.82 nm) for 28 days (6-h/day, 5-days/week for four weeks) either with separate NP inhalation exposures or with combined co-exposure in a nose-only inhalation system. Mass concentrations sampled from the breathing zone were AuNP $19.34 \pm 2.55 \mu\text{g}/\text{m}^3$ and AgNP $17.38 \pm 1.88 \mu\text{g}/\text{m}^3$ for separate exposure and AuNP $8.20 \mu\text{g}/\text{m}^3$ and AgNP $8.99 \mu\text{g}/\text{m}^3$ for co-exposure. Lung retention and clearance were previously determined on day 1 (6-h) of exposure (E-1) and on post-exposure days 1, 7, and 28 (PEO-1, PEO-7, and PEO-28, respectively). In addition, the fate of nanoparticles, including translocation and elimination from the lung to the major organs, were determined during the post-exposure observation period.

Results AuNP was translocated to the extrapulmonary organs, including the liver, kidney, spleen, testis, epididymis, olfactory bulb, hilar and brachial lymph nodes, and brain after subacute inhalation and showed biopersistence regardless of AuNP single exposure or AuNP + AgNP co-exposure, showing similar elimination half-time. In contrast, Ag was translocated to the tissues and rapidly eliminated from the tissues regardless of AuNP co-exposure. Ag was continually accumulated in the olfactory bulb and brain and persistent until PEO-28.

Conclusion Our co-exposure study of AuNP and AgNP indicated that soluble AgNP and insoluble AuNP translocated differently, showing soluble AgNP could be dissolved into Ag ion to translocate to the extrapulmonary organs and rapidly removed from most organs except the brain and olfactory bulb. Insoluble AuNPs were continually translocated to the extrapulmonary organs, and they were not eliminated rapidly.

Keywords Biokinetics, Toxicokinetics, Translocation, Silver nanoparticles, Gold nanoparticles, Elimination, Tissue distribution, Clearance, Co-inhalation exposure

*Correspondence:

Günter Oberdörster

Gunter_Oberdorster@URMC.Rochester.edu

Il Je Yu

u1670916@chol.com

Full list of author information is available at the end of the article



© The Author(s) 2023. **Open Access** This article is licensed under a Creative Commons Attribution 4.0 International License, which permits use, sharing, adaptation, distribution and reproduction in any medium or format, as long as you give appropriate credit to the original author(s) and the source, provide a link to the Creative Commons licence, and indicate if changes were made. The images or other third party material in this article are included in the article's Creative Commons licence, unless indicated otherwise in a credit line to the material. If material is not included in the article's Creative Commons licence and your intended use is not permitted by statutory regulation or exceeds the permitted use, you will need to obtain permission directly from the copyright holder. To view a copy of this licence, visit <http://creativecommons.org/licenses/by/4.0/>. The Creative Commons Public Domain Dedication waiver (<http://creativecommons.org/publicdomain/zero/1.0/>) applies to the data made available in this article, unless otherwise stated in a credit line to the data.

Background

Nanoparticles have been known to be translocated to other organs after exposure and eliminated from the organs. Major exposure pathways are through inhalation, ingestion, or injection. The lung-deposited aerosol state nanoparticles are readily translocated to extrapulmonary organs and other target organs by different routes and mechanisms. One is systemic blood circulation or via lymphatic ducts after crossing the air–liquid barrier to the respiratory epithelial layer and interstitial tissues. Another is by sensory nerve endings in the airway epithelia, followed by axonal translocation to ganglionic and CNS structures [1]. Previously, other groups have demonstrated two different pathways of clearance from the lung that exist after subacute co-exposure of soluble silver nanoparticles (AgNP) and insoluble gold nanoparticle (AuNP) and thereafter post-exposure observation (PEO) period. Insoluble AuNP is mechanically cleared, while soluble AgNP is cleared initially chemically by dissolution and by mechanically after the dissolved Ag ions form insoluble secondary AgNP with biogenic molecules [2–5]. The clearance mechanisms for inhaled solid particles in the respiratory tract are physical clearance processes (translocation), including mucociliary movement, macrophage phagocytosis, epithelial endocytosis, lymphatic drainage, blood circulation, and sensory neurons, and chemical clearance processes including dissolution, leaching, and protein binding [1].

Translocation or tissue distribution of AgNP after inhalation exposure has been studied, exhibiting wide tissue distribution [6–10]. Several lung retention studies after AgNP inhalation suggest that AgNP which is soluble can be existed as AgNP, Ag ion and secondary insoluble AgNP in the lung [2–4]. Extrapulmonary translocation or tissue distribution of AuNP after inhalation also showed wide tissue distribution to a less degree than AgNP [3, 11–14]. Workers in the workplace and consumers using nanomaterial-containing products are not likely to be exposed to one kind of nanomaterials; rather, they could be co-exposed to multiple nanoparticles, including soluble and insoluble nanomaterials. Lung retention and clearance of co-inhalation exposure of soluble nanoparticles AgNP and insoluble nanoparticles AuNP have been studied in a previous study by Kim et al. [3]. The study indicated that the clearance of AgNPs follows a two-compartment model of fast and slow dissolution rates, while the clearance of AuNPs could be described by a one-compartment model with a longer half-time. The co-exposure of AuNPs + AgNPs showed that the clearance of AgNPs was altered by the presence of AuNPs, perhaps due to some interaction between AgNP and AuNP affecting dissolution and/or mechanical clearance of AgNP in vivo [3].

Extrapulmonary translocation of AgNP and AuNP after co-inhalation exposure of AgNP and AuNP has not been studied; furthermore, the elimination of AgNP and AuNP from the organs after co-inhalation exposure also has not been studied. Understanding the translocation and clearance of insoluble nanoparticles such as AuNP and soluble nanoparticles such as AgNP after co-inhalation exposure will enhance our knowledge of the toxicokinetics of nanomaterials. Thus, the aim of this paper is to show that insoluble AuNPs and soluble AgNPs after inhalation alone or in combination is their translocation to extrapulmonary organs and thereafter their elimination. Also, the effect of one particle type on the other on these processes upon co-exposure. In this report, we have investigated the fate of translocated AgNP and AuNP after co-exposure.

Results

Characterization of AgNP and AuNP aerosols in inhalation chambers

The total number concentrations, count median diameter (CMD), geometric standard deviation (GSD), and surface area of the AgNPs, AuNPs, and AuNPs + AgNPs measured by the DMAS during the exposure period are published and presented in Additional file 1: Table S1 [3]. FE-TEM revealed non-agglomerated particles, and TEM-EDS identified AgNP and AuNP particles in each chamber (Additional file 1: Figure S1) [3]. The mass concentrations analyzed by AAS via filter sampling were $17.38 \pm 1.88 \mu\text{g}/\text{m}^3$ for AgNPs, $19.34 \pm 2.55 \mu\text{g}/\text{m}^3$ for AuNPs for single exposure, and $8.99 \pm 1.77 \mu\text{g}/\text{m}^3$ for AuNPs + $8.20 \pm 1.05 \mu\text{g}/\text{m}^3$ for AuNP + AgNP for co-exposure, while the mass concentrations estimated by DMAS were $10.12 \pm 0.71 \mu\text{g}/\text{m}^3$ for AgNPs and $17.68 \pm 1.1.69 \mu\text{g}/\text{m}^3$ for AuNPs, respectively. TEM indicated that the AgNPs, AuNPs, and AuNPs + AgNPs were the particle diameters log-normally distributed between 6 and 30 nm. The CMD and GSD measurements were 10.40 nm and 1.36, respectively, for the AuNPs, 9.48 nm and 1.49, respectively, for the AgNPs, and 9.00 nm and 1.19, respectively, for the AuNP + AgNP coexposure (Additional file 1: Table S1, Fig. S2).

Organ retention after AuNP exposure and AuNP + AgNP co-exposure

Our previous study [2] investigated the lung burden of rats that were exposed to biosoluble silver nanoparticles (AgNPs, 10.86 nm) and to biopersistent gold nanoparticles (AuNPs, 10.82 nm) for 28 days (6-h/day, 5-days/week for 4 weeks) either with separate NP inhalation exposures or with combined co-exposure. After 28-day of AuNP or AuNP + AgNP coexposure, a 97.9 and 97.1% of Au were retained, respectively (Additional file 1: Table S2). For

Single AuNP exposure, an elimination half-time ($T_{1/2}$) was 81.5 days, while coexposure with AgNP reduced the AuNP $T_{1/2}$ to 54.2 days (Table 1).

Organ concentrations of Au and Ag after subacute exposure and post-exposure observation (PEOs) periods were presented in Table 2 and 3, respectively. AuNP was continually accumulated in the lung with very low elimination during the subacute exposure period of either AuNP alone or AuNP + AgNP coexposure. Liver, kidney, and hilar lymph nodes showed a considerable amount of extrapulmonary translocation of AuNP (Table 2). Other organs, including the spleen, testis epididymis, thymus, olfactory bulb, brachial lymph node, brain, eye, and blood, showed very low translocation with sub-nanogram ranges (Fig. 1). Comparing the hilar lymph node to the brachial lymph node, the lymphatic translocation of AuNP showed increased translocation of AuNP proximal to the lung compared with distal to the lung. As seen in Fig. 1, AuNPs exposed either AuNP alone (AuNP E-1, closed triangle) or together with AgNP (AuNP + AgNP E1, open triangle) were continually accumulated in the extrapulmonary organs from the exposure 1-day (E-1) to post-exposure 1-day (PEO-1). AuNPs were either eliminated slowly from the tissues or accumulated in the most examined organs, including the liver ($T_{1/2}$ 192.6 days for AuNP exposure; 221.4 days coexposure), kidney, Spleen ($T_{1/2}$ 177 days), testis, epididymis, and brain, either after 28-days of AuNP single exposure (closed circle) or AuNP + AgNP coexposure (open circle) (Table 1, Fig. 1, Table 2). The kidney, spleen testis, and epididymis showed accumulation of Au with AuNP alone and AuNP + AgNP

coexposure. The eyes, brachial lymph node, hilar lymph node, and olfactory bulb showed a persistent tissue concentration of Au after AuNP or AuNP + AgNP coexposure. The accumulated AuNPs were not easily cleared from most organs, including the liver, kidney, spleen testis, epididymis, hilar lymph nodes, and brain (Table 1, Fig. 1, Table 2). The kidney, spleen, testis, and epididymis showed accumulation of Au alone or with AgNP. The olfactory bulb, eyes, brachial lymph nodes, and thymus showed some level of clearance with AuNP exposure but not with AgNP coexposure, even after PEO-28. These organs showing somewhat faster elimination compared with slower elimination organs could be due to the small number of samples, the lower concentration (<ng), and the resulting deviation. When the AuNP elimination was plotted with organ elimination kinetics, Au elimination in the liver, kidney, spleen, epididymis, olfactory bulb, eye, and brachial lymph node showed similar elimination regardless of AuNP exposure alone or AuNP + AgNP coexposure (Table 2, Additional file 1: Fig. S3). Other organs, such as the hilar lymph node, testis, thymus, and brain, showed different retention between AuNP alone and AuNP + AgNP coexposure. Interestingly, the brain exposed to AuNP alone showed V-shaped elimination kinetics showing reduced retention at PEO-7, but the retention increased again at PEO-28 (Additional file 1: Fig. S3). The hilar lymph node, the first organ of translocation from the lung except blood, showed a different pattern showing increased retention of PEO-7 and PEO-28 when comparing AuNP alone with AuNP + AgNP coexposure, indicating continuous translocation of AuNP

Table 1 Elimination half-times ($T_{1/2}$) of Au and Ag in organs (days)

Exposure	AuNP (days)	AuNP + AgNP (days)	AgNP (days)	AuNP + AgNP (days)
Measured	Au		Ag	
Lung*	81.5	54.2	3.1 (fast) 48.5 (slow)	2.2 (fast) 28.4 (slow)
Liver	192.60	221.4	1.4	2.5
Kidneys	Accumulation	Accumulation	Accumulation	Accumulation
Spleen	177.0	Accumulation	Accumulation	NE
Testes	NE	Accumulation	Accumulation	Accumulation
Epididymis	Accumulation	Accumulation	29.9 days	Accumulation
Olfactory bulb	20.4	NE	75.1	17.8
Eyes	25.8	NE	68.7	128.6
Brain	NE	NE	Accumulation	108.9
Hilar lymph nodes	65.3	25.2	11.4	2.8
Brachial lymph nodes	10.8	11.1	59.7	53.5
Thymus	17.7	NE	89.5	Accumulation
Blood	2.2	NE	NE	NE

NE, not eliminated; Accumulated, Au or Ag concentration is increased during PEO

*Kim et al. [3]

Table 2 (continued)

	Eye	Blood
PEO1	0.079 ± 0.014	0.001 ± 0.000
PEO7	0.065 ± 0.016	0.053 ± 0.017
PEO 28	0.047 ± 0.011	0.005 ± 0.003

A statistics analysis was used Anova and test.

A, samples were analyzed using by ICP-MS and calculated following $\text{ppb} \times \text{final volume (5 mL)} \times \text{dilution factor (10 times)} / \text{organ weight}$.

B, Organ weights were measured using by micro balance. Before measure weight, washed blood to di-water and wiped up to paper.

C, The gold concentration $(\text{ng/g}) \times \text{organ weight (g)}$; N/D was analyzed sample silver concentration lower than compare with control.

Statistics were analyzed Anova (multiple comparison analysis) and t-test. This result was described in Table that Anova was from a to cc and t-test was * and **.

^a $P < 0.05$, compared with PEO-1 and PEO-7

^b $P < 0.05$, compared with PEO-1 and PEO-28

^{aa} $P < 0.01$, compared with PEO-1 and PEO-7

^{bb} $P < 0.01$, compared with PEO-1 and PEO-28

* $P < 0.05$, compared with PEO-1 and PEO-7

** $P < 0.01$, compared with PEO-1 and PEO-28

Table 3 The organ distribution for silver after inhaled of AgNP at exposure 1 day (E-1), post-exposure observation 1 day (PEO-1), PEO-7 days and PEO-28 days (mean ± S.E.; 4 animals of exposure 1 day; 5 animals of PEO-1, PEO-7 and PEO-28). A statistics analysis was used Anova and test

AgNP	Liver				Kidney				Spleen				Testis				Epididymis					
	ng/g ^a	Organ wt (g) ^b	Au/organ (ng) ^c	ng/g ^a	Organ wt (g) ^b	Au/organ (ng) ^c	ng/g ^a	Organ wt (g) ^b	Au/organ (ng) ^c	ng/g ^a	Organ wt (g) ^b	Au/organ (ng) ^c	ng/g ^a	Organ wt (g) ^b	Au/organ (ng) ^c	ng/g ^a	Organ wt (g) ^b	Au/organ (ng) ^c	ng/g ^a	Organ wt (g) ^b	Au/organ (ng) ^c	
E-1	7.981 ± 1.458	8.767 ± 0.332	69.407 ± 11.214	0.767 ± 0.223	1.175 ± 0.061	0.926 ± 0.327	N/D	0.657 ± 0.131	N/D	0.261 ± 0.130	1.488 ± 0.174	0.344 ± 0.142	N/D	0.339 ± 0.022	N/D							
PEO1	7.235 ± 1.907	9.418 ± 0.467	66.974 ± 18.033*	0.486 ± 0.266	1.192 ± 0.043	0.623 ± 0.376	0.724 ± 0.493	0.600 ± 0.013	0.426 ± 0.118	0.284 ± 0.083	1.511 ± 0.086	0.431 ± 0.126	0.166 ± 0.030	0.506 ± 0.035	0.078 ± 0.014 ^a							
PEO7	0.215 ± 0.149	10.717 ± 0.430	2.573 ± 1.593	0.444 ± 0.444	1.330 ± 0.053	0.575 ± 0.575	1.279 ± -	0.723 ± 0.040	0.836 ± -	0.195 ± 0.082	1.550 ± 0.108	0.257 ± 0.112	0.641 ± 0.218	0.624 ± 0.065	0.359 ± 0.112 ^{ab}							
PEO 28	N/D	11.768 ± 0.180	N/D	N/D	1.449 ± 0.056	N/D	N/D	0.972 ± 0.068	N/D	0.168 ± 0.168	1.677 ± 0.046	0.277 ± 0.272	0.102 ± 0.010	0.610 ± 0.047	0.062 ± 0.008							
Co-exposure	Liver				Kidney				Spleen				Testis				Epididymis					
	ng/g ^a	Organ wt (g) ^b	Au/organ (ng) ^c	ng/g ^a	Organ wt (g) ^b	Au/organ (ng) ^c	ng/g ^a	Organ wt (g) ^b	Au/organ (ng) ^c	ng/g ^a	Organ wt (g) ^b	Au/organ (ng) ^c	ng/g ^a	Organ wt (g) ^b	Au/organ (ng) ^c	ng/g ^a	Organ wt (g) ^b	Au/organ (ng) ^c	ng/g ^a	Organ wt (g) ^b	Au/organ (ng) ^c	
E-1	2.238 ± 0.628	9.362 ± 1.021	22.598 ± 8.612	0.198 ± -	1.226 ± 0.110	0.244 ± -	N/D	0.589 ± 0.074	0.166 ± 0.044	N/D	1.528 ± 0.044	N/D	N/D	0.296 ± 0.012	N/D							
PEO1	4.912 ± 1.988	9.237 ± 0.529	42.262 ± 14.830	0.372 ± 0.155	1.257 ± 0.037	0.469 ± 0.190	1.832 ± 0.197	0.571 ± 0.023	0.999 ± 0.099	0.199 ± 0.050	1.638 ± 0.089	0.313 ± 0.069	0.008 ± 0.008	0.482 ± 0.058	0.004 ± 0.004							
PEO7	0.894 ± 0.673	9.987 ± 0.919	7.098 ± 4.499	0.375 ± -	1.300 ± 0.074	0.537 ± -	0.699 ± 0.111	0.656 ± 0.043	0.492 ± 0.126	0.279 ± 0.061	1.611 ± 0.087	0.476 ± 0.125	0.235 ± 0.077	0.550 ± 0.051	0.125 ± 0.046							
PEO 28	N/D	13.905 ± 0.894	N/D	N/D	1.609 ± 0.053	N/D	N/D	1.054 ± 0.142	N/D	0.132 ± -	1.677 ± 0.021	0.211 ± -	0.327 ± 0.070	0.675 ± 0.080	0.213 ± 0.076							
AgNP	Thymus				Olfactory bulb				Hilar lymph node				Brachial lymph node				Brain					
	ng/g ^a	Organ wt (g) ^b	Au/organ (ng) ^c	ng/g ^a	Organ wt (g) ^b	Au/organ (ng) ^c	ng/g ^a	Organ wt (g) ^b	Au/organ (ng) ^c	ng/g ^a	Organ wt (g) ^b	Au/organ (ng) ^c	ng/g ^a	Organ wt (g) ^b	Au/organ (ng) ^c	ng/g ^a	Organ wt (g) ^b	Au/organ (ng) ^c	ng/g ^a	Organ wt (g) ^b	Au/organ (ng) ^c	
E-1	N/D	0.597 ± 0.050	N/D	2.842 ± 1.175	0.044 ± 0.008	0.098 ± 0.030	62.109 ± 8.273	0.004 ± 0.001	0.206 ± 0.039	3.009 ± 1.858	0.044 ± 0.008	0.095 ± 0.048	N/D	2.093 ± 0.015	N/D							
PEO1	N/D	0.471 ± 0.098	N/D	25.646 ± 4.401	0.059 ± 0.002	1.552 ± 0.303	16.337 ± 13.087	0.014 ± 0.003	0.196 ± 0.157	8.119 ± 4.437	0.059 ± 0.002	0.495 ± 0.279	1.219 ± 0.151	2.049 ± 0.061	2.507 ± 0.336							
PEO7	0.482 ± -	0.497 ± 0.031	0.280 ± -	24.925 ± 3.328	0.063 ± 0.003	1.559 ± 0.200	4.055 ± 1.298	0.042 ± 0.006	0.146 ± 0.044	18.072 ± 9.080	0.063 ± 0.003	1.152 ± 0.504	0.941 ± 0.121	2.192 ± 0.040	2.045 ± 0.231							
PEO 28	N/D	0.393 ± 0.034	N/D	19.160 ± 0.567	0.065 ± 0.004	1.245 ± 0.108	N/D	0.033 ± 0.006	N/D	7.073 ± 5.843	0.065 ± 0.004	0.387 ± 0.306	1.195 ± 0.115	2.147 ± 0.046	2.568 ± 0.262							
Co-exposure	Thymus				Olfactory bulb				Hilar lymph node				Brachial lymph node				Brain					
	ng/g ^a	Organ wt (g) ^b	Au/organ (ng) ^c	ng/g ^a	Organ wt (g) ^b	Au/organ (ng) ^c	ng/g ^a	Organ wt (g) ^b	Au/organ (ng) ^c	ng/g ^a	Organ wt (g) ^b	Au/organ (ng) ^c	ng/g ^a	Organ wt (g) ^b	Au/organ (ng) ^c	ng/g ^a	Organ wt (g) ^b	Au/organ (ng) ^c	ng/g ^a	Organ wt (g) ^b	Au/organ (ng) ^c	
E-1	0.146 ± -	0.573 ± 0.043	0.146 ± -	1.180 ± 0.394	0.061 ± 0.008	0.065 ± 0.026	15.323 ± 6.319	0.019 ± 0.005	0.105 ± 0.068	N/D	0.061 ± 0.008	N/D	N/D	2.093 ± 0.015	N/D							
PEO1	0.958 ± 0.279	0.430 ± 0.055	0.277 ± 0.044	9.369 ± 2.395	0.103 ± 0.008	0.916 ± 0.192 ^b	11.537 ± 6.950	0.022 ± 0.005	0.143 ± 0.079	0.192 ± -	0.103 ± 0.008	0.018 ± -	0.284 ± 0.105	2.079 ± 0.023	0.593 ± 0.221							
PEO7	0.252 ± -	0.498 ± 0.044	0.152 ± -	4.443 ± 0.786	0.108 ± 0.008	0.484 ± 0.105	0.242 ± -	0.034 ± 0.004	0.004 ± -	0.303 ± -	0.108 ± 0.008	0.035 ± -	0.752 ± 0.280	2.118 ± 0.062	1.536 ± 0.553							
PEO 28	N/D	0.466 ± 0.044	N/D	3.302 ± 0.378	0.111 ± 0.008	0.372 ± 0.061	N/D	0.050 ± 0.005	N/D	N/D	0.111 ± 0.008	N/D	0.510 ± 0.151	2.277 ± 0.032	1.144 ± 0.322							
AgNP	Eye				Blood																	
	ng/g ^a	Organ wt (g) ^b	Au/organ (ng) ^c	ng/g ^a	Organ wt (g) ^b	Au/organ (ng) ^c																
E-1	0.989 ± 0.509	0.333 ± 0.005	0.320 ± 0.161	0.027 ± 0.004	0.5	0.013 ± 0.004																
PEO1	0.218 ± -	0.355 ± 0.017	0.083 ± -	0.036 ± 0.008	0.5	0.018 ± 0.004*																
PEO7	1.253 ± 0.211	0.389 ± 0.007	0.476 ± 0.091	0.004 ± 0.002	0.5	0.002 ± 0.001																
PEO 28	0.077 ± -	0.419 ± 0.016	0.034 ± -	N/D	0.5	N/D																

Table 3 (continued)

Co-exposure	Eye			Blood	
E-1	N/D	0.334 ± 0.020	N/D	0.008 ± 0.001	0.5
PEO1	N/D	0.376 ± 0.016	N/D	0.016 ± 0.002	0.5
PEO7	N/D	0.370 ± 0.006	N/D	0.004 ± 0.001	0.5
PEO-28	N/D	0.561 ± 0.090	N/D	0.008 ± 0.001	0.5

A. samples were analyzed using by ICP-MS and calculated following ppb (ug/L) x final volume (5 mL) x dilution factor (10 times) / organ weight.

B. Organ weights were measured using by micro balance. Before measure weight, washed blood to di-water and wiped up to paper.

C. The silver concentration (ng/g) x organ weight (g)

N/D was analyzed sample silver concentration lower than compare with control.

A statistics were analyzed Anova (multiple comparison analysis of Dennett test) and t-test. This result was described in Table that Anova was from a to cc and t-test was * and **.

Where (Anova)

^a P < 0.05, compared with PEO-1 and PEO-7

^b P < 0.05, compared with PEO-1 and PEO-28

^{aa} P < 0.01, compared with PEO-7 and PEO-28

Where (t-test)

*P < 0.05, and **P < 0.01

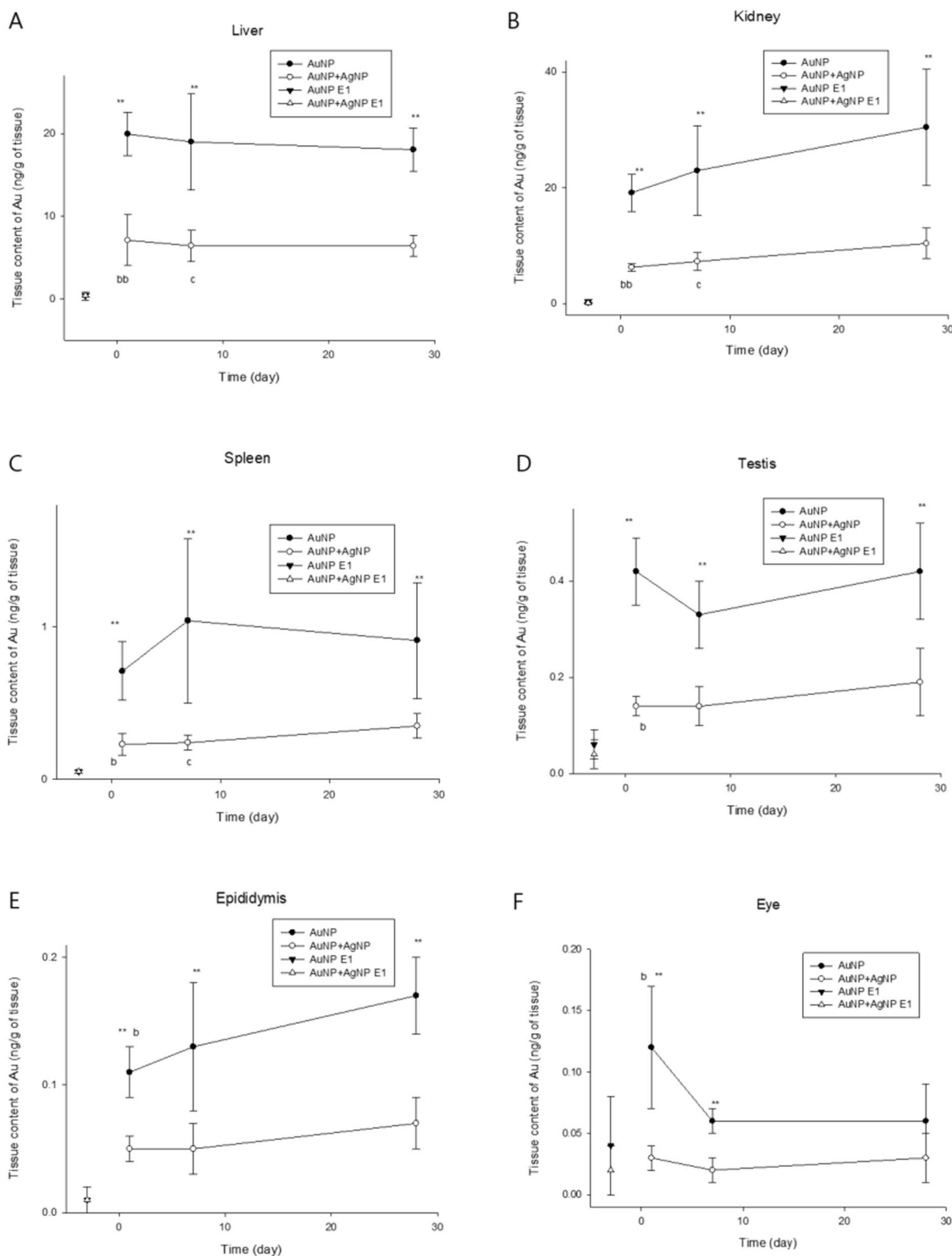


Fig. 1 Tissue Au concentration after 28-day inhalation exposure and post exposure period. E1, exposure 1 day. ^b*P* < 0.05, compared with PEO-1 and PEO-28; ^c*P* < 0.05, compared with PEO-7 and PEO-28; ^{bb}*P* < 0.01, compared with PEO-1 and PEO-28; Where (t-test) **P* < 0.05, and ***P* < 0.01

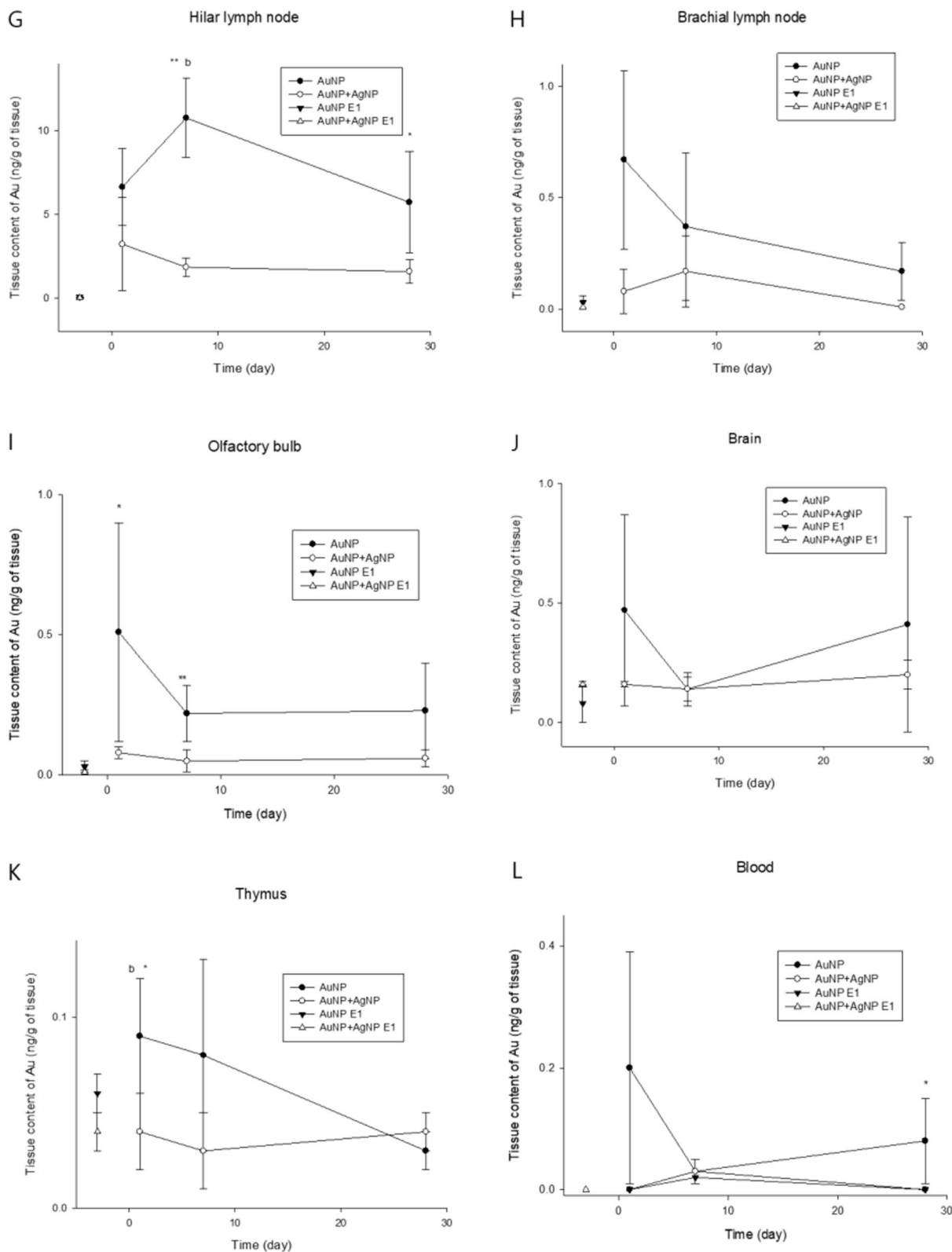


Fig. 1 continued

from the lung tissue to the lymph node even after termination of inhalation exposure (Fig. 1).

AgNP exposure and AgNP and AuNP co-exposure

In contrast to AuNP exposure, between 34 and 49% of deposited Ag in the lung was estimated to be solubilized and removed from the lung within 5 days after 28-days of AgNP exposure and AuNP-AgNP co-exposure. Estimated insoluble AgNPs were retained at 66.1% and 51.2% after 28-days of AgNP and AgNP + AuNP co-exposure, respectively (Additional file 1: Table S2). The elimination of single AgNP exposure and AuNP + AgNP co-exposure showed two phases for Ag elimination; fast and slow. The fast-elimination $T_{1/2}$ after single exposure was 3.1 days, and the slow-elimination $T_{1/2}$ single exposure was 48.5 days. AuNP + AgNP co-exposure also showed 2 phases of Ag elimination in the lung; fast and slow, where the fast-elimination $T_{1/2}$ was 2.2 days, and the slow-elimination $T_{1/2}$ was 28.4 days (Table 1).

Compared with AuNP exposure, in which AuNPs were continually accumulated in the organ during 28-days of inhalation exposure and eliminated AuNP very slowly thereafter or accumulated in some tissues, AgNP exposure showed a somewhat different pattern from AuNP. The liver showed a noticeable amount of Ag that was translocated from the lung but eliminated very fast, showing $T_{1/2}$ 1.4 days for AgNP exposure and 2.5 days for AuNP co-exposure (Table 1). The olfactory bulb and brain also showed a significant amount of translocation compared with other organs (Table 3). As shown in Fig. 2, the similar levels of Ag in the organs at E-1 comparing the levels of Ag at PEO-1 indicated that Ag in the organs was rapidly cleared from the organs. Liver ($T_{1/2}$ 1.4 days for AgNP and 2.5 days for co-exposure) (Table 1), kidney, spleen, testis, epididymis, eye, hilar and brachial lymph nodes, and thymus showed rapid elimination of Ag from the tissue. Although the kidney, spleen, epididymis, hilar and brachial lymph nodes, and thymus showed somewhat long elimination, the levels of tissue concentration of Ag at E-1 are lower and similar to levels of PEO-1. Despite the fact that elimination half-time ($T_{1/2}$) was estimated in these organs, the tissue concentration of these tissues was so small (< ng) to make any conclusions. Therefore, a small amount of Ag was translocated, and Ag may not be accumulated in those tissues. In contrast, the olfactory bulb and brain showed an accumulation of Ag in the organs during the post-observation period (Table 3, Additional file 1: Fig. S4). Testis and brain showed a trend of accumulation of Ag during the PEOs. The retention of Ag in most organs was not affected by the co-exposure of AuNP, except for some statistical differences in the spleen at PEO-1 and olfactory bulb at PEO-7 and 28 (Fig. 2, Table 3, Additional file 1: Fig. S4).

Discussion

In the present work, we have studied extrapulmonary translocation and retention of Au and Ag after subacute inhalation exposure to AuNP or AgNP single exposure or AuNP + AgNP co-exposure and thereafter post-exposure observation (PEO) period. Earlier studies have shown that the inhaled AgNP was cleared from the lung by a two-phase mode, fast and slow, while AuNPs were cleared by a one-phase mode [2, 3]. The inhaled AuNP and AgNP were detected in the extrapulmonary organs were analyzed by ICP-MS. Since AuNP is insoluble, AuNP will be in the form of AuNP form. Ag translocated to the extrapulmonary organs could be either Ag ions, AgNP, or secondary AgNP, produced by silver ions reacting with biomolecules [2, 3, 5]. Whichever form AgNPs are translocated from the lung, and Ag measured in the extrapulmonary tissue were rapidly cleared from the tissues except for the olfactory bulb and brain, evidenced by similar concentration levels with under nanogram ranges between Ag levels in the E-1 and Ag levels in the PEOs. Therefore, Ag showed increased retention in the olfactory bulb and brain.

Both AuNP or AgNP can also be translocated to the extrapulmonary organs by ingestion through the gastrointestinal (GI) tract by mucociliary escalation, blood or lymphatic circulation, or through the olfactory bulb. Most organs having the reticuloendothelial system (RES), such as the liver, spleen, kidney, and lymph node, retain AuNP longer time, and they may not be eliminated fast. Furthermore, organs having a biological barrier, such as the testis and brain, also retain insoluble AuNPs or insoluble AgNP. Our subacute study indicated that the translocated AuNP might not be cleared at all in most organs.

Our previous subacute inhalation study on AuNP and AgNP single exposure and AuNP + AgNP co-exposure indicated that insoluble AuNPs were eliminated slowly from the lung, showing $T_{1/2}$ 81.5 days, while soluble AgNP showed two modes of fast ($T_{1/2}$ 3.1 days) and slow ($T_{1/2}$ 48.5 days) [3]. We do not know which forms of AgNP (e.g. AgNP, Ag ion, and secondary AgNP) are translocated to extrapulmonary organs, yet a particular form of AgNP could be translocated with a low level, as seen from AuNP translocation. Our previous study on the lung retention toxicokinetic study suggested that the ionic silver form, which is eliminated rapidly from the lung, could be easily translocated to extrapulmonary organs [3]. The organs with the reticuloendothelial system, such as the liver, kidney, spleen, and lymph node, did not show long-term retention of AgNP, as seen in AuNP. Therefore, major forms of AgNP translocated to the extrapulmonary organs are silver ions which are rapidly eliminated from the organs, as seen in the liver. The most secondary AgNP generated from Ag ion

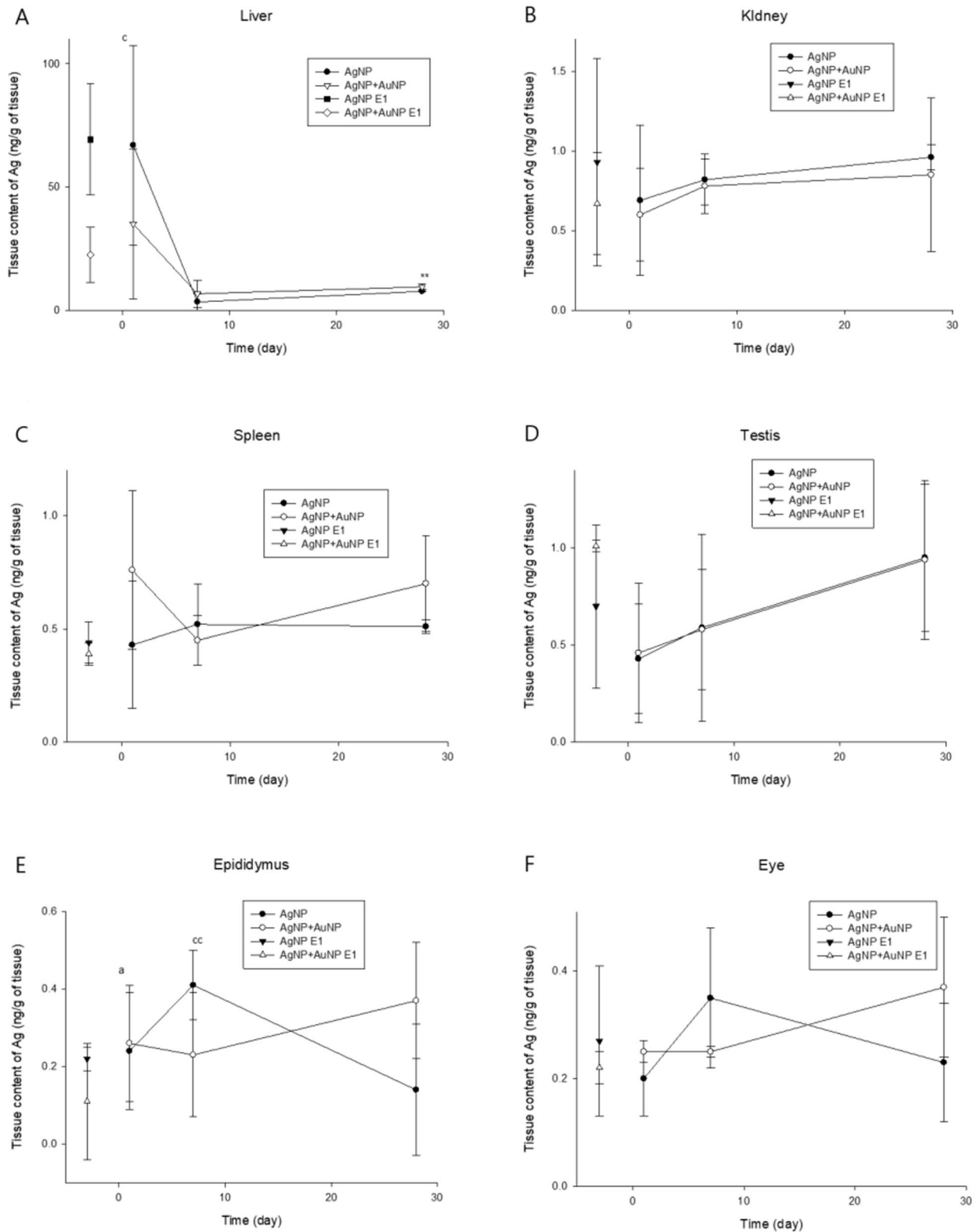


Fig. 2 Tissue Ag concentration after 28-day inhalation exposure and post exposure period. ^a*P* < 0.05, compared with PEO-1 and PEO-7; ^b*P* < 0.05, compared with PEO-1 and PEO-28; ^c*P* < 0.05, compared with PEO-7 and PEO-28; ^{cc}*P* < 0.01, compared with PEO-7 and PEO-28; Where (t-test) **P* < 0.05, and ***P* < 0.01

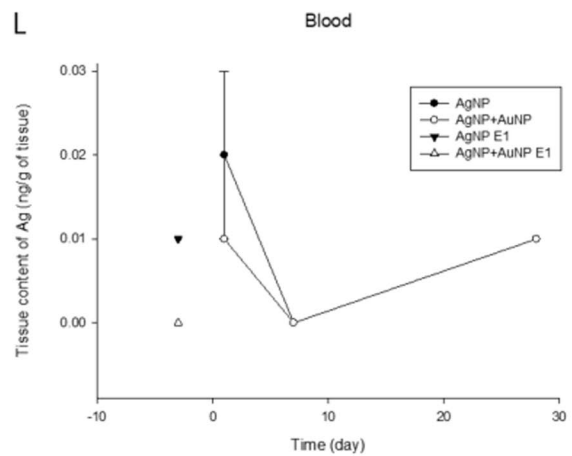
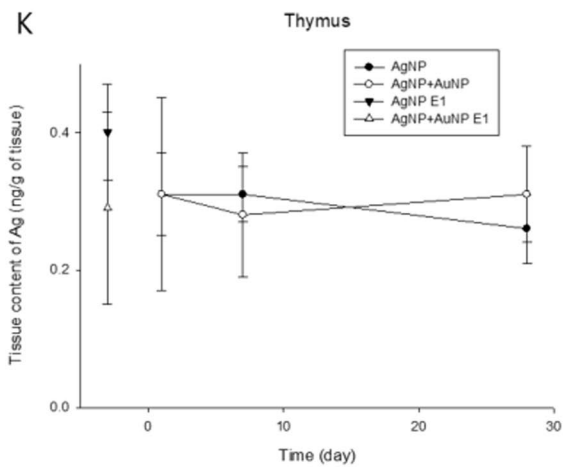
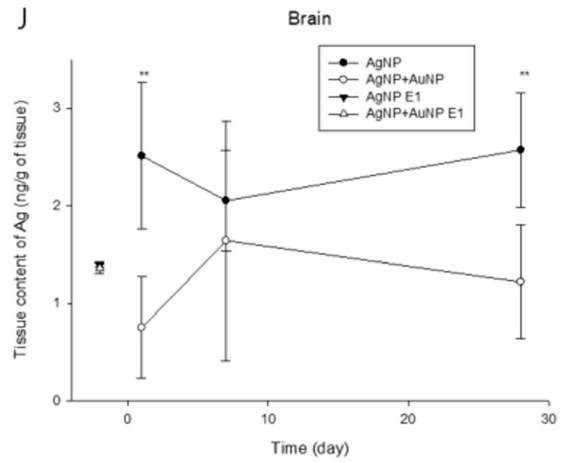
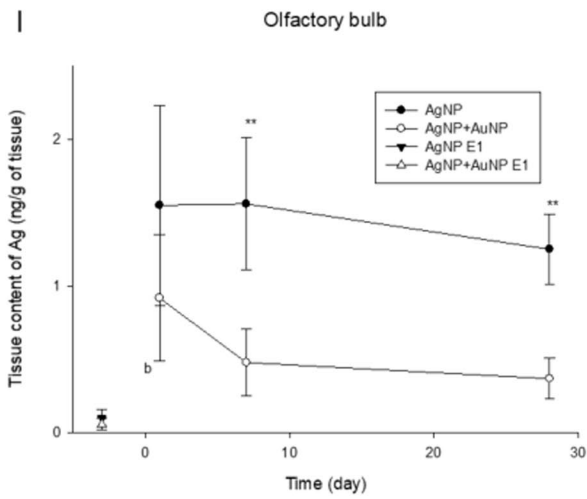
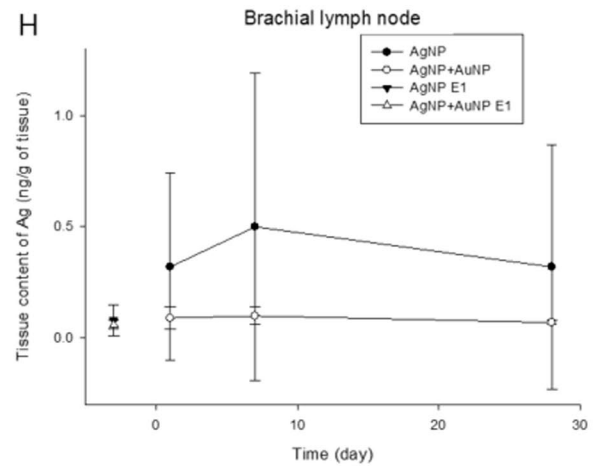
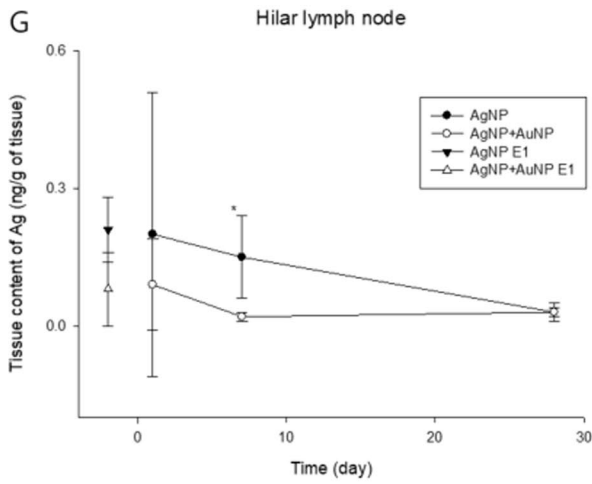


Fig. 2 continued

reacting with biomolecules in the lung could be cleared slowly from the lung with a long half-life. On the other hand, organs having biological barriers, such as the testis and brain, may transform Ag ions to insoluble secondary AgNPs and retain insoluble AgNPs long-term. Or insoluble AgNPs may be translocated to these organs. The olfactory system also acts as a direct portal for AgNP to the brain. Previous our 12-week AgNP inhalation and 4-week and 12-week recovery study at a concentration of 49, 117, and 381 $\mu\text{g}/\text{m}^3$ also showed rapid clearance of Ag from the liver, kidneys, and spleen and long-term retention of Ag in the brain [8].

Our other study on tissue distribution and clearance of AuNP (12.8 nm) and AgNP (10 nm) single exposure and co-exposure after subacute intravenous (IV) injection and thereafter PEO-28 recovery [15] showed similar features as well as quite different features compared with the current inhalation study. Au concentration in the tissues did not clear, as seen in Ag after 4-weeks of recovery, showing biopersistence or accumulation in the liver, kidneys, spleen, and brain after PEO-28. Co-administration of AgNP + AuNP resulted in a mutual reduction of their tissue distribution with possible competitive inhibition, and these nanoparticles could be distributed to the organs in particulate forms instead of ionic forms. These IV co-administration study results showed some similarity in the biopersistence in the tissues for AuNPs with the co-inhalation exposure study but a difference in competition in the tissue distribution, while the co-inhalation study showed independent distribution and clearance from the tissues. The absorption process in the portal of exposure may likely influence this difference. Nanoparticles are deposited in the lungs and dissolved into ions and formed into secondary nanoparticles in the case of AgNP before being distributed to extrapulmonary organs through systemic circulation or lymphatic duct. Or some AgNPs inhaled were delivered to the GI tract by mucociliary escalator absorbing to the liver by the portal vein. Rapid elimination of Ag in the liver could be due to the elimination of Ag ionic form. Moreover, AuNPs or secondary AgNPs should be able to cross the air-blood barrier and the basal lamina to reach systemic circulation. In the case of IV injection, nanoparticles can be distributed to tissues without processing and crossing these barriers. Although it is not an AuNP + AgNP co-administration study, our previous study on AgNP (10 nm) 28-day oral administration study with 100 mg/kg and 500 mg/kg body weight and thereafter 4-month recovery showed gradual clearance from the liver, kidneys, and spleen due to high dose comparing with inhalation, but biopersistence to the testis and brain [16]. Therefore, the route of administration and amount of dosing can influence tissue distribution and clearance of nanoparticles.

Conclusions

AgNPs, (10.86 nm) and AuNPs, (10.82 nm) were exposed to male rats for 28 days (6-h/day, 5-days/week for four weeks) either with separate NP inhalation exposures or with combined co-exposure in a nose-only inhalation system. Extrapulmonary translocation from the lung and elimination from the major extrapulmonary organs were determined on day one and on post-exposure days 1, 7, and 28 (PEO-1, PEO-7, and PEO-28). AuNP was translocated to the extrapulmonary organs, including the liver, kidney, spleen, testis, epididymis, olfactory bulb, hilar and brachial lymph nodes, and brain after subacute inhalation and showed biopersistence regardless of AuNP single exposure or AuNP + AgNP co-exposure, showing similar elimination half-time. Ag was translocated to the extrapulmonary tissues and rapidly eliminated from the tissues regardless of AuNP co-exposure. Ag was continually accumulated in the olfactory bulb and brain and persistent until PEO-28. The co-exposure study of AuNP and AgNP indicated that soluble AgNP and insoluble AuNP translocated differently, showing soluble AgNP could be dissolved into Ag ion to translocate to the extrapulmonary organs and rapidly removed from most organs except the brain and olfactory bulb. Insoluble AuNPs were continually translocated to the extrapulmonary organs, and they were not eliminated rapidly.

Materials and methods

AuNP and AgNP aerosol generation

The method of co-inhalation exposure of AuNP and AgNP has been published [3]. The nano-aerosol generator consisted of a small ceramic heater connected to an AC power supply that was housed within a quartz tube furnace. The heater dimensions were $50 \times 5 \times 1.5$ mm, and a surface temperature of about 1500 °C within a local heating area of 5×10 mm² was achieved within about 10 s. For long-term testing, the source materials (about 160 mg), silver wire (100 mg, 99.99% purity, 0.5 mm diameter, Higglab Co., Ltd, Korea), and gold wire (70 mg, 99.99% purity, 0.5 mm diameter, Higglab Co., Ltd, Korea), were positioned in a separate ceramic heater at the highest temperature point. The quartz tube was 70 mm in diameter and 140 mm in length. Clean (dry and filtered) air was used as the carrier gas, and the gas flow was maintained at 25.0 L/min ($Re=572$, laminar flow regime) using a mass flow controller (MFC, AERA, FC-7810CD-4 V, Japan) [6–8, 17]. In the current study, the exposure system consisted of four nose-only chambers; fresh air control, AgNP exposure, AuNP exposure, and AuNP + AgNP co-exposure (Additional file 1: Fig. S5). Each generator used 4–5 Lpm (liters per minute), and the remaining air flows of AgNP, AuNP, and AuNP + AgNP were 25.1 ± 0.10 Lpm, 24.8 ± 0.15 , and 24.2 ± 0.1 Lpm

(AgNP 11.9 ± 0.12 Lpm / AuNP 12.3 ± 0.11 Lpm), respectively. The total airflow in each chamber was 35 Lpm, controlled by the mass flow controller. The airflow from the generators was divided by a valve controller into the AgNP, AuNP, and AuNP + AgNP exposure chambers (NITC, HCT, Icheon, Korea). The target nanoparticle diameter was 10 nm for each nanoparticle exposure, and the target mass concentrations for the AgNP, AuNP, and AuNP + AgNP exposures were $20 \mu\text{g}/\text{m}^3$, $20 \mu\text{g}/\text{m}^3$, and $10 \mu\text{g}/\text{m}^3$ AgNP + $10 \mu\text{g}/\text{m}^3$ AuNP, respectively [3].

Monitoring of inhalation chambers and analysis of AgNPs and AuNPs

In each chamber, the nanoparticle size distribution, including the count median diameter (CMD), geometric standard deviation (GSD), particle number, volume, and predicted surface area, were recorded using a differential mobility analyzer system (DMAS) comprised of a differential mobility analyzer (DMA-20, 4220, range 6–225 nm, HCT Co., Ltd. Korea) and condensation particle counter (CPC, 3775, size range 4 nm–1 μm , TSI INC., Shoreview, MN). Nanoparticles from 6 to 225 nm were measured using sheath air at 15 L/min and polydispersed aerosol air at 1.5 L/min for the DMAS with a density of $10.49 \text{ g}/\text{cm}^3$ for Ag and $19.32 \text{ g}/\text{cm}^3$ for Au, respectively. In addition, the mass concentrations of AgNP and AuNP were determined chemically by using an atomic absorption spectrophotometer (AAS, Perkin-Elmer 900 T, Waltham, MA, USA) after sampling on a mixed cellulose ester (MCE) filter (size: 37 mm and pore size 0.45 μm , SKC, UK) at a flow rate of 1.0 L/min and digesting the samples on a hot plate (PerkinElmer, Concord, ON, Canada) using nitric acid (Fluka, Lot; BCBM5181V). Two samples collected daily from each chamber were analyzed during the 28-day exposure period.

Transmission electron microscopy (TEM)

The AgNPs, AuNPs, and AuNPs + AgNPs were collected on a TEM grid (electron microscope, 200 mesh, Formvar/Carbon, TEDpella, CA) and imaged for morphology using a field emission transmission electron microscope (FE-TEM, JEM2100F, 200 kV, JEOL, Tokyo, Japan). Their chemical composition was analyzed using an energy-dispersive X-ray analyzer (EDX, TM200, Oxford Instruments PLC, Oxfordshire, UK), while the CMD and GSD were obtained after measuring 200 particles for each.

Animal care and housing conditions

Seventy-six male 6-week-old specific-pathogen-free Sprague–Dawley rats (average body weight 178.53 ± 0.63 g) were purchased from OrientBio (Seongnam, Korea) and

acclimated for one week before commencing the experiments. Three to four rats were housed in polycarbonate cages during the acclimation and experimental period. The animal room temperature, humidity, and light/dark cycle were 21.40 ± 0.55 °C, $48.67 \pm 5.56\%$, and 12 h, respectively. Filtered water and a rodent diet (BSC, Republic of Korea) were supplied ad libitum. The rats were adapted to the nose-only tubes for a week with daily tube placement for 2 h. The 7-week-old rats weighing 273.63 ± 2.83 g were divided into four groups: fresh air control, AgNP, AuNP, and AuNP + AgNP exposure groups, and exposed 6-h/day, 5 days/week for four weeks. Each exposure group included 19 animals (4 rats for day-1 (6-h) exposure and five rats for 1-day, 7-days, and 28-days post-exposure sacrifices, respectively). The animals were examined daily on weekdays for any evidence of exposure-related effects, including respiratory, dermal, behavioral, nasal, or genitourinary changes suggestive of irritation. The body weights were evaluated at the time of purchase, at the time of grouping, once a week during the inhalation exposure and post-exposure period, and before necropsy (results are not shown). The rat experiments were approved by the Hanyang University Institutional Animal Care and Use Committee in South Korea (HY-IACUC-2017-0143A).

Immediately after the 6-h exposure on days 1 and 1, 7, and 28 days after the 28-day exposure period, rats were sacrificed by anesthetizing via an intraperitoneal injection of pentobarbital (EntobarVR, Hanlim Pharm Co. Ltd., Seoul, Korea) at a dose of 150 mg/kg body weight. The animals in the control group were sacrificed first, and all the dissection instruments were thoroughly washed with 70% ethyl alcohol in between the dissections to avoid NP contamination from one organ to another. Blood was drawn from the abdominal aorta for exsanguination. Lungs, liver, kidneys, spleen, testis, epididymis, thymus, hilar lymph node, bronchial lymph node, olfactory bulb, brain, and eyes were selected. After measuring the organ weights, the organs were fixed with 10% neutral buffer formalin for further processing. An aliquot of the fixed organs was then digested as described in NIOSH 7302 [18] using a microwave (MARS 230/60, CEM, Matthews, NC) with the following three steps: (1) increase the temperature to 110 °C for 15 min; (2) maintain this temperature for 60 min (1600 w); and (3) cool for 15 min. The digestion solution for lung tissue consisted of 2 mL of nitric acid (purity of 69.0%; CAS. No of 7697–37-2, Fluka, Germany), and 3 mL of 1% nitric acid to make a final volume of 5 ml. The samples were then analyzed using an inductively coupled plasma mass spectrometer (ICP-MS, PerkinElmer NEXION 300S, Concord, ON, Canada). The ICP-MS analysis was conducted according to NIOSH 8200 [19]. The concentrations of Ag and Au in the organs were determined by ICP-MS based on standard

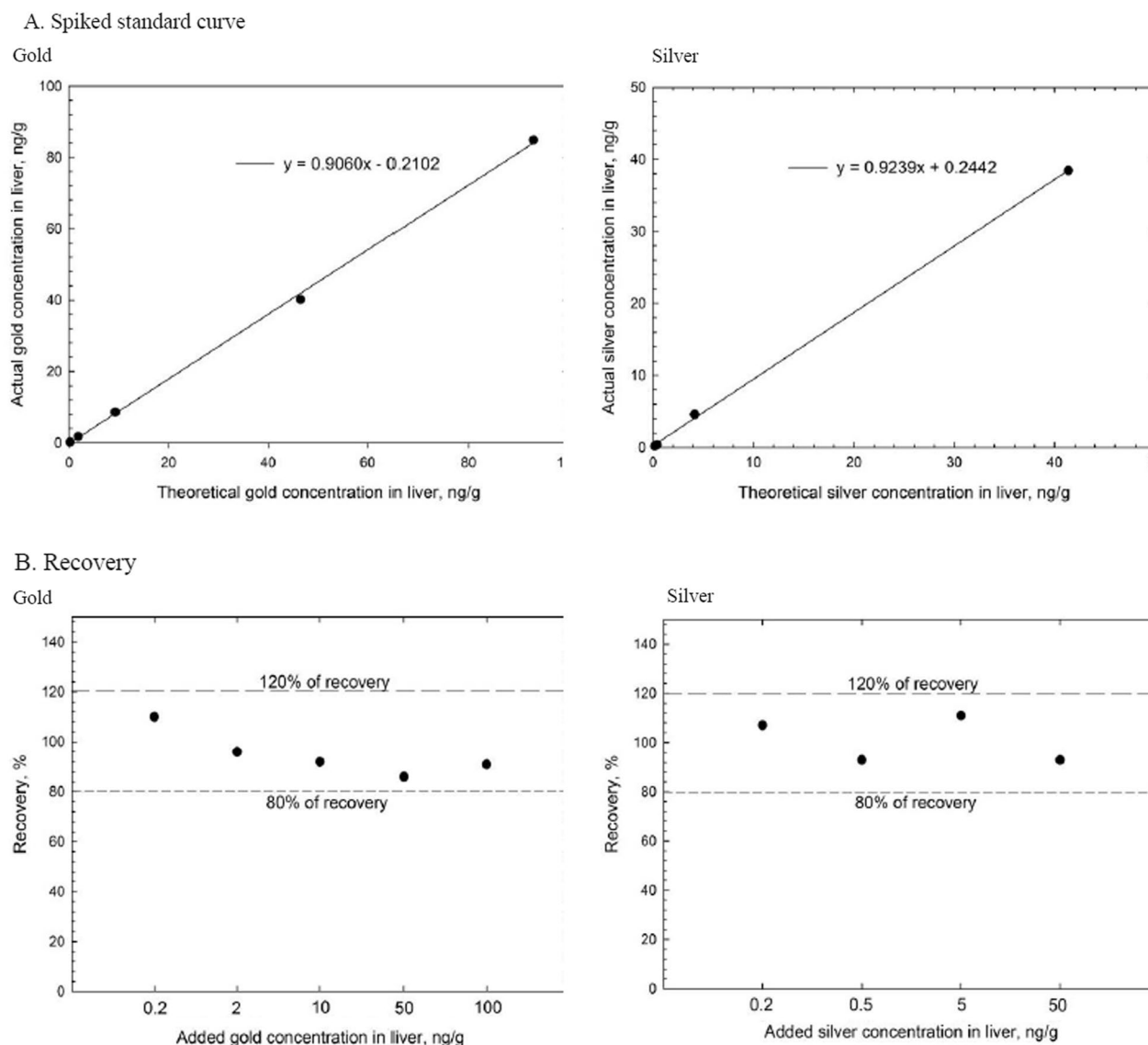


Fig. 3 Spiked standard curve and recovery for gold and silver in liver. **A**, Spiked standard curve ranges were analyzed gold of 0.2–100 ng/g and silver of 0.2–50 ng/g. **B**, this measured gold recovery of 91–110% and silver recovery of 93–111%

curves established with un-exposed clean livers spiked with test NPs sampled from the respective inhalation chambers, where the results from digestion, extraction, and dilution were all performed in duplicates. The quantitative analyses for Ag and Au in the liver were corrected using the spiked standard curve. The recovery yields of AgNPs and AuNPs were 81 – 113% and 84 – 105%, respectively, as shown in Fig. 3. The spiked standard curves ranged from 0.2 – 5 ng/g of liver tissue for AgNPs and 2–100 ng/g of lung tissue for AuNPs. When analyzing the samples, the dilution factor was 100 times. The digestion recovery of AgNPs and AuNPs in the liver tissue was calculated using Eq. 1

$$\text{Recovery (\%)} = \frac{\text{measured concentration (ng/g)}}{\text{spiked concentration (ng/g)}} \times 100 \tag{1}$$

The mass content of nanoparticles in the organ was calibrated using the weight of the organ. The samples were all analyzed using a standard calibration curve that ranged from 0.05 – 0.5 ppb for Ag and 1–10 ppb for Au. After analyzing standard blanks 40 times, the measured LOD and LOQ were 0.086 µg /L and 0.260 µg /L, respectively, for Ag and 0.027 µg /L and 0.082 µg/L, respectively, for Au.

Organ retention, translocation, and elimination kinetics

The organ elimination kinetics for the AgNPs, AuNPs, and AuNP + AgNP co-exposure were determined based on lung burdens measured on 1-day (6-h) of exposure (E-1) and on post-exposure observation days 1 (PEO-1), 7 (PEO-7), and 28 (PEO-28). The fraction of organ concentration per initial organ concentration at PEO-1 was used for estimating retention, translocation, and clearance kinetics for PEO-7 and PEO-28, applying an appropriate-order clearance model. The fractions of organ concentration at PEO-1 (i.e. PEO-1/PEO-1, PEO-7/PEO-1 and PEO-28/PEO-1) were plotted as Y-axis, and PEO periods were plotted as the X-axis. The -order model is described by Eq. 2. The retention half-time () was derived using 1, 2, and natural log (2), as shown in Eq. (3).

$$M(t) = P \exp(-\lambda t) \quad (2)$$

where

- $M(t)$; lung burden at time (t)
- P ; fraction of lung burden cleared (1.0 for one-compartment model)
- λ ; clearance rate per day for one-compartment model

$$T_{1/2} = \frac{\ln(2)}{\lambda} \approx \frac{0.693}{\lambda} \quad (3)$$

Statistical analysis

An analysis of variance (ANOVA) test and Dunnett T3 multi-range tests were used with up to two points, where one point compared the single and co-exposure groups, while two points compared each group from PEO-1 to PEO-28. The level of significance was set at $P < 0.05$.

Supplementary Information

The online version contains supplementary material available at <https://doi.org/10.1186/s12989-023-00515-z>.

Additional file 1. Table S1: Aerosol data for AuNPs, AgNPs, and AuNP + AgNP co-exposure (From Table 1 of Kim et al. [3]). **Figure S1:** FE-TEM analysis for AgNPs, AuNPs, and AgNP + AuNP co-exposure in chambers [3]; A, image of single AgNP (scale 20 nm); B, EDS result for single AgNP; C, image of single AuNP (scale 20 nm); D, EDS result for single AuNP; E, image of AgNP + AuNP co-exposure (scale 100 nm); F, EDS result for AgNP + AuNP co-exposure. **Figure S2:** Particle distribution in exposure chambers based on DMAS and FE-TEM [3]; (A), CMD and GSD using DMAS during exposure period; (B), Particle diameter using DMAS; (C), CMD and GSD for AgNPs using FE-TEM; (D), CMD and GSD for AuNPs using FE-TEM; (E) CMD and GSD for AgNP + AuNP co-exposure using FE-TEM. **Table S2:** Lung burden of AuNPs, AgNPs and AuNP + AgNPs co-exposure (ng/lung). **Figure S3:** Au retention after 28-day inhalation exposure and post-exposure period. **Figure S4:** Au retention after 28-day inhalation exposure and post-exposure period. **Figure S5:** Schematic of exposure system for generating AuNPs, AgNPs, and AuNP + AgNP co-exposure for nose only exposure chambers [3]

Author contributions

P.L., experimental and manuscript preparation; J.K.K., experimental preparation; M.S.J., Ag and Au ICP analysis; H.P.K., aerosol monitoring; K.H.A., aerosol technology advice and manuscript review; J.D.P., advice and manuscript review; M.G., advice and manuscript review; G.O. and I.J.Y., experimental planning, manuscript preparation and review. All authors read and approved the final manuscript.

Funding

This study was supported by the Global Top Environment Technology Development project (No. 2018001860004) funded by the Ministry of Environment.

Availability of data and materials

All data and materials are included in the manuscript, tables, figures and supplements. The datasets during and/or analyzed during the current study are available from the corresponding author on reasonable request.

Declarations

Ethics approval and consent to participate

The study was carried out in agreement with Korean Animal Welfare Act. The study was approved by the Hanyang University's Institutional Animal Care and Use Committee (2017-0134A).

Consent for publication

Not applicable.

Competing interests

The authors declare that they have no competing interests.

Author details

¹Institute for Genomics, Biocomputing and Biotechnology, Starkville, MS, USA. ²HCT CO., LTD, Seoicheon-Ro 578 Beon-Gil, Majang-Myeon, Icheon 17383, Korea. ³Hanyang University, Ansan, Korea. ⁴College of Medicine, Chung-Ang University, Seoul, Korea. ⁵Haematology and Molecular Medicine, University of the Witwatersrand, Johannesburg, South Africa. ⁶Water Research Group, Unit for Environmental Sciences and Management, North-West University, Potchefstroom, South Africa. ⁷Department of Environmental Medicine, University of Rochester, Rochester, NY, USA.

Received: 30 September 2022 Accepted: 24 January 2023

Published online: 31 March 2023

References

1. Oberdorster G, Oberdorster E, Oberdorster J. Nanotoxicology: an emerging discipline evolving from studies of ultrafine particles. *Environ Health Perspect*. 2005;113(7):823–39.
2. Jo MS, Kim JK, Kim Y, Kim HP, Kim HS, Ahn K, Lee JH, Faustman EM, Gulumian M, Kelman B, Yu IJ. Mode of silver clearance following 28-day inhalation exposure to silver nanoparticles determined from lung burden assessment including post-exposure observation periods. *Arch Toxicol*. 2020;94(3):773–784.
3. Kim JK, Kim HP, Park JD, Ahn K, Kim WY, Gulumian M, Oberdorster G, Yu IJ. Lung retention and pharmacokinetics of silver and gold nanoparticles in rats following subacute inhalation co-exposure. *Part Fibre Toxicol*. 2021;18:5.
4. Kreyling WG, Möller W, Holzwarth U, Hirn S, Wenk A, Schleh C, Schäffler M, Haberl N, Gibson N, Schittny JC. Age-dependent rat lung deposition patterns of inhaled 20 nanometer gold nanoparticles and their quantitative biokinetics in adult rats. *ACS Nano*. 2018;12:7771–90.
5. Kreyling WG, Holzwarth U, Hirn S, Schleh C, Wenk A, Schäffler M, Haberl N, Gibson N. Quantitative biokinetics over a 28 day period of freshly generated, pristine, 20 nm silver nanoparticle aerosols in healthy adult rats after a single 1½-hour inhalation exposure. *Part Fibre Toxicol*. 2020;17:21.
6. Ji JH, Jung JH, Kim SS, Yoon JU, Park JD, Choi BS, Chung YH, Kwon IH, Jeong J, Han BS, Shin JH, Sung JH, Song KS, Yu IJ. Twenty-eight-day inhalation toxicity study of silver nanoparticles in Sprague Dawley Rats. *Inhalation Toxicol*. 2007;19(10):857–871.

7. Sung JH, Ji JH, Park JD, Yoon JU, Kim DS, Jeon KS, Song MY, Jeong J, Han BS, Han JH, Chung YH, Chang HK, Lee JH, Cho MH, Kelman BJ, Yu IJ. Subchronic inhalation toxicity of silver nanoparticles. *Toxicol Sci*. 2009;108(2):452–61.
8. Song KS, Sung JH, Ji JH, Lee JH, Lee JS, Ryu HR, Lee JK, Chung YH, Park HM, Shin BS, Chang HK, Kelman B, Yu IJ. Recovery from silver-nanoparticle-exposure-induced lung inflammation and lung function changes in sprague dawley rats. *Nanotoxicology*. 2013;7(2):169–80.
9. Braakhuis HM, Gosens I, Krystek P, Boere JA, Cassee FR, Fokkens PH, Post JA, van Loveren H, Park MV. Particle size dependent deposition and pulmonary inflammation after shortterm inhalation of silver nanoparticles. *Part Fibre Toxicol*. 2014;11:49.
10. Anderson DS, Patchin ES, Silva RM, Uyeminami DL, Sharmah A, Guo T, Das GK, Brown JM, Shannahan J, Gordon T, Chen LC, Pinkerton KE, Van Winkle LS. Influence of particle size on persistence and clearance of aerosolized silver nanoparticles in the rat lung. *Toxicol Sci*. 2015;144(2):366–73.
11. Seiffert J, Buckley A, Leo B, Martin NG, Zhu J, Dai R, Hussain F, Guo C, Warren J, Hodgson A, Gong J, Ryan MP, Zhang JJ, Porter A, Tetley TD, Gow A, Smith R, Chung KF. Pulmonary effects of inhalation of spark-generated silver nanoparticles in Brown-Norway and Sprague-Dawley rats. *Respir Res*. 2016;17(1):85.
12. Takenaka S, Karg E, Kreyling WG, Lentner B, Moller W, Behnke-Semmler M, Jennen L, Walch A, Michalke B, Schramel P, Heyder J, Schulz H. Distribution pattern of inhaled ultrafine gold particles in the rat lung. *Inhalation Toxicol*. 2006;18:733–40.
13. Sung JH, Ji JH, Park JD, Song MY, Song KS, Ryu HR, Yoon JU, Jeon KS, Jeong J, Han BS, Chung YH, Chang HK, Lee JH, Kim DW, Kelman BJ, Yu IJ. Subchronic inhalation toxicity of gold nanoparticles. *Part Fibre Toxicol*. 2011;8(1):16.
14. Han SG, Lee JS, Ahn K, Kim YS, Kim JK, Lee JH, Shin JH, Jeon KS, Cho WS, Song NW, Gulumian M, Shin BS, Yu IJ. Size-dependent clearance of gold nanoparticles from lungs of Sprague-Dawley rats after short-term inhalation exposure. *Arch Toxicol*. 2015;89(7):1083–94.
15. Lee JH, Sung JH, Ryu HR, Song KS, Song NW, Park HM, Shin BS, Ahn K, Gulumian M, Faustman EM, Yu IJ. Tissue distribution of gold and silver after subacute intravenous injection of co-administered gold and silver nanoparticles of similar sizes. *Arch Toxicol*. 2018;92(4):1393–405.
16. Lee JH, Kim YS, Song KS, Ryu HR, Sung JH, Park JD, Park HM, Song NW, Shin BS, Marshak D, Ahn K, Lee HE, Yu IJ. Biopersistence of silver nanoparticles in tissues from Sprague-Dawley rats. *Part Fibre Toxicol*. 2013;10:36.
17. Ji JH, Jung JH, Yu IJ, Kim SS. Long-term stability characteristics of metal nanoparticle generator using small ceramic heater for inhalation toxicity studies. *Inhalation Toxicol*. 2007;19:745–51.
18. NIOSH (National Institute for Occupational Safety and Health). NIOSH Manual of Analytical Method 7302. Elements by ICP (Microwave digestion). NIOSH, Cincinnati. 2014.
19. NIOSH (National Institute for Occupational Safety and Health). NIOSH Manual of Analytical Method 8200. Elements in Tissues. NIOSH, Cincinnati. 2018.

Publisher's Note

Springer Nature remains neutral with regard to jurisdictional claims in published maps and institutional affiliations.

Ready to submit your research? Choose BMC and benefit from:

- fast, convenient online submission
- thorough peer review by experienced researchers in your field
- rapid publication on acceptance
- support for research data, including large and complex data types
- gold Open Access which fosters wider collaboration and increased citations
- maximum visibility for your research: over 100M website views per year

At BMC, research is always in progress.

Learn more biomedcentral.com/submissions

